Per. Mineral. (1999), *68*, 3, 287-313

PERIODICO di MINERALOGIA
established in 1930

An International Journal of
MINERALOGY, CRYSTALLOGRAPHY, GEOCHEMISTRY, ORE DEPOSITS, PETROLOGY, VOLCANOLOGY
and applied topics on *Environment, Archaeometry* and *Cultural Heritage*

Zeolitic occurrences from Tertiary pyroclastic flows and related epiclastic deposits outcropping in northern Sardinia (Italy)

PAOLA MORBIDELLI[1], MARIA ROSARIA GHIARA[2]*, ROBERTO LONIS[3] and ANTONIO SAU[3]

[1] Dipartimento di Scienze della Terra, Università "La Sapienza", P.le Aldo Moro 5, I-00185 Roma, Italy
[2] Dipartimento di Scienze della Terra, Università "Federico II", Via Mezzocannone 8, I-80134 Napoli, Italy
[3] Progemisa, S.p.A., Via Contivecchi 7, I-09122 Cagliari, Italy

Submitted, July 1999 - Accepted, November 1999

ABSTRACT. — This study is part of research work aimed at identifying zeolitic occurrences of economic interest in Sardinia.

The aim of the present work is to define genetic models for zeolite occurring in Tertiary pyroclastic flows outcropping in northern Sardinia (Logudoro region). The sample area, covering about 1000 km^2, includes the villages of Ozieri, Ploaghe, Ittireddu, Chilivani, Mores and Bonorva.

The most important volcanic formations, outcropping here, include the oldest manifestations (24-15 Ma) of Oligo-Miocene orogenic magmatism in Sardinia. Tertiary volcanics include poorly welded (ILP and IC) and welded (IS) ash and pumice flows; epiclastic (EV and EN) and base surge (BS) deposits are locally interbedded. Field research, devoted to lithostratigraphic reconstruction of outcropping suites, also showed numerous degassing pipes inside ignimbritic rocks.

Laboratory research identified various rock components (matrix, phenocrysts, pumice and xenoliths) and modal analyses were also carried out near Bonorva. The distributive and textural features of secondary minerals (zeolite, smectite, silica minerals and glauconite) were also examined. Microscopic (optical and SEM) data defined the following crystallization order:

smectite ⇒ clinoptilolite ⇒ opal-CT ⇒ mordenite.

The most common zeolitic variety is clinoptilolite, which: 1) fills vugs and degassing pipe structures; 2) lines both tubular and sub-spherical vesicles in pumice; 3) grows on cuspate glassy fragments; 4) intergrows with silica minerals in patches randomly distributed in the matrix; 5) constitutes the felt-form intergrowths of well-developed crystals growing on the matrix; 6) lines veins which, in the central part, are filled with anhedral calcitic aggregates.

The overall data set suggests the following three genetic models for this zeolitic material: *a*) crystallization from fluids entrapped inside sub-spherical vesicles hosted in pumiceous fragments; *b*) crystallization linked to polyphase tranformation of glassy components by juvenile fluids and *c*) crystallization linked to interaction processes on glassy components by external fluids.

RIASSUNTO. — Questo studio si inserisce in una ricerca volta all'individuazione di siti caratterizzati dalla presenza di adunamenti zeolitici di interesse economico in Sardegna.

La presente ricerca mira alla ricostruzione delle modalità genetiche delle zeoliti in funzione delle loro diverse giaciture nei flussi piroclastici di età Terziaria affioranti nella Sardegna centro settentrionale in corrispondenza del Logudoro.

Il settore preso in esame ha un'estensione di circa 1000 km^2 e comprende gli abitati di Ozieri, Ploaghe, Ittireddu, Chilivani, Mores e Bonorva. In questa zona, le formazioni vulcaniche volumetricamente

* Corresponding author, E-mail: mghiara@unina.it.

più importanti sono riferibili alle manifestazioni più antiche (24-15 Ma) del magmatismo Oligo-Miocenico. Si tratta di flussi piroclastici pomiceo-cineritici poco saldati (ILP e IC) e saldati (IS) che formano estese piattaforme costituite dalla sovrapposizione di varie unità di raffreddamento; talora si ritrovano intercalati livelli di materiale epiclastico (EV, EN) e prodotti di *base surges* (BS).

Le indagini di campagna, miranti alla ricostruzione litostratigrafica delle unità affioranti, hanno permesso di rilevare la presenza di camini di degassamento distinguibili anche sotto il profilo mineralogico. Si è proceduto, quindi, all'individuazione anche quantitativa (areale di Bonorva) delle componenti delle rocce (matrice, fenocristalli, pomici ed inclusi litoidi) ed all'analisi della distribuzione e delle giaciture dei minerali secondari (zeoliti, smectiti, minerali della silice e glauconite). Lo studio microscopico, ottico ed al SEM, ha evidenziato il seguente ordine di cristallizzazione:

smectite ⇒ clinoptilolite ⇒ opale-CT ⇒ mordenite.

Le zeoliti decisamente meglio rappresentate e, spesso uniche, sono le clinoptiloliti che: 1) tappezzano i vacuoli ed i condotti di degassazione; 2) riempiono parzialmente o circondano le vescicole delle pomici; 3) si impostano e crescono su frammenti vetrosi; 4) crescono a chiazze sulla matrice cineritica; 5) crescono alle salbande di vene contenenti, talora, nella porzione centrale, calcite e 6) si rinvengono in vene cementanti fratture imputabili al raffreddamento del flusso piroclastico.

L'insieme dei dati emersi ha permesso di proporre tre modelli genetici: *a*) deposizione a spese di fluidi intrappolati all'interno delle vescicole delle pomici; *b*) cristallizzazione correlabile a processi di interazione tra fluidi juvenili e componente vetrosa; *c*) cristallizzazione correlabile a processi di interazione tra fluidi non juvenili e componente vetrosa.

KEY WORDS: *Zeolites, clinoptilolite, transformation processes, Sardinia, pyroclastic flows, epiclastite, base surge deposits.*

INTRODUCTION AND GEOLOGICAL SETTING

Zeolite-bearing ignimbrites of possible commercial value have recently been recognized in northern Sardinia (Italy) (Ghiara *et al.*, 1995; de' Gennaro *et al.*, 1995). Zeolites occur in Tertiary poorly welded ash and pumice pyroclastic flows, forming thick deposits and large plateaux, mainly filling the Sardinian Rift system (Lecca *et al.*, 1997).

The rhyodacitic ignimbrites are part of orogenic volcanism which developed between 28 and 16 Ma (Lecca *et al.*, 1997, and references therein), characterized by a close field association of basaltic to andesitic lavas and ignimbrites. The climax of activity, according to Beccaluva *et al.* (1985) and Lecca *et al.* (1997), occurred from 23 to 17 Ma in concomitance with the rotation of the Sardinia-Corsica microplate (21-19.5 Ma; Montigny *et al.*, 1981). The earlier volcanic manifestations (28-24 Ma) are some subvolcanic bodies (Calabona, Monte Nurecci and Sarroch districts) and the lower andesitic sequences of Capo Marrargiu, Monastir, Furtei, and part of the Arcuentu complex (Lecca *et al.*, 1997; Brotzu *et al.*, 1997). These magmatic products are locally overlain by lower Aquitanian marine sediments (Cherchi, 1985).

As regards ignimbritic deposits, radiometric and stratigraphic data indicate that they are confined to 24-15 Ma; the lowermost ignimbrites, represented by small outcrops of whitish ash and pumice pyroclastic flows, outcrop along the western Sardinian coast (Funtanazza and Bosano areas) and in the north-western zone of the Sardinia Rift near Pianu Ladu (Logudoro). The youngest ignimbrites (about 16 Ma) are mainly located in southern Sardinia, where they are covered by Serravallian-Messinian marine deposits (Lecca *et al.*, 1997). The climax of explosive activity is confined to 21-19 Ma.

Previous studies (Ghiara *et al.*, 1997) on zeolites occurring in the poorly welded ash and pumice pyroclastic flows from northern Sardinia indicate that:

– most of the zeolites belong to the heulandite-clinoptilolite serie;

– among the zeolites, clinoptilolite is the most abundant, followed by mordenite;

– exstensive random variations in zeolite contents occur in both overlapping cooling units and within single cooling units;

– large variations occur in the extra-framework cation contents of zeolites;

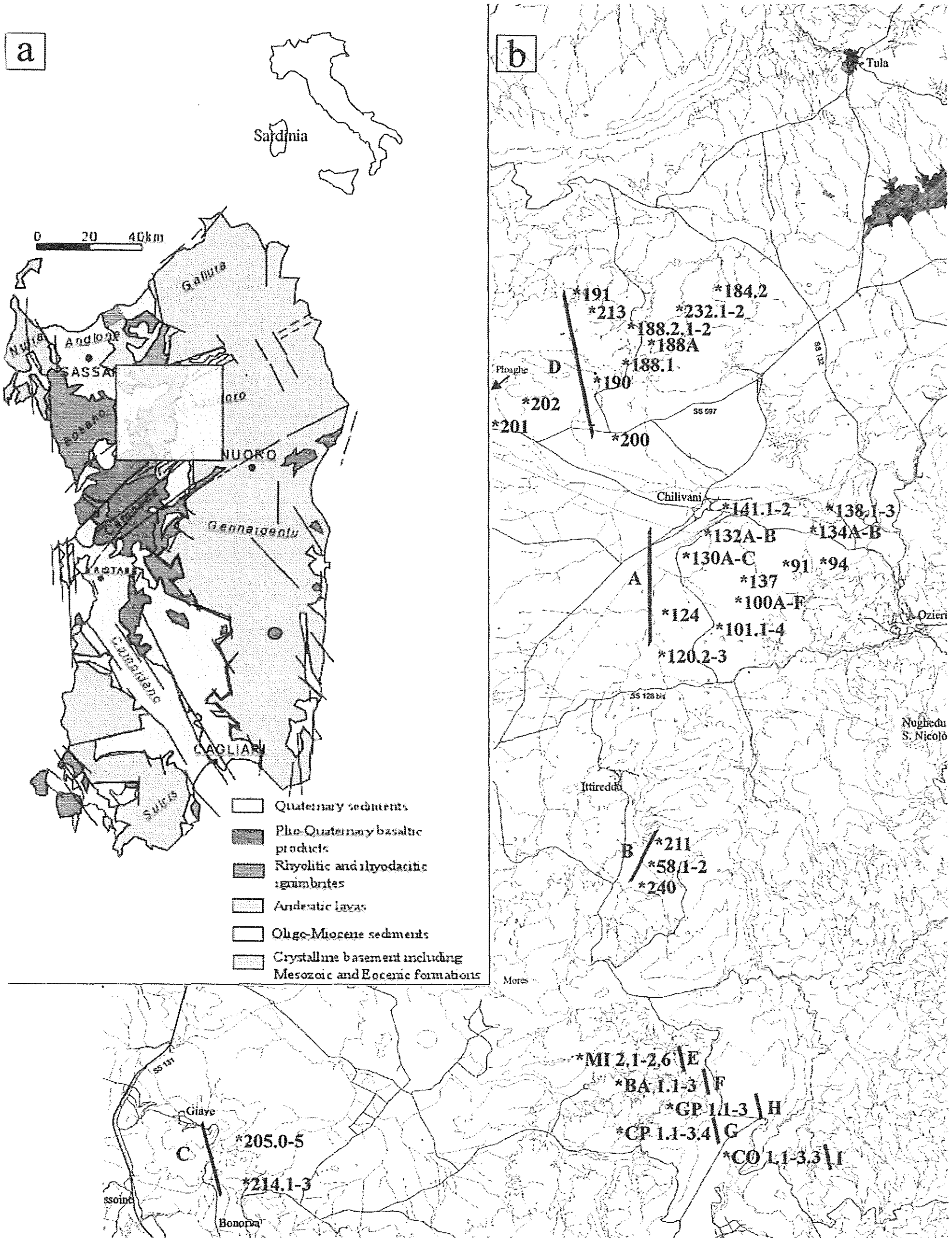

Fig. 1 – *a*) Structural sketch map of Sardinia (from Cherchi and Montadert, 1982 and Savelli *et al.*, 1979; simplified) showing Oligo-Miocene Rift system; study area is expanded in *b*).
b) Location of samples used to reconstruct the following stratigraphic sequences: A=Monte Mainas; B=Monte S. Bernardo; C=Monte Fulcadu; D=Sant'Antonio di Bisarcio; E=Monte Inzos (MI); F=Badiamenta (BA); G=Case Pinna (CP); H=Giolzi Perra (GP); I=Case Oddorai (CO).

– zeolites are closely associated with other secondary minerals, mainly represented by smectite and opal-CT.

At present, there is no conclusive minerogenetic model for these zeolites. The dominant role of the fluid gaseous component from pyroclastic flows in zeolite crystallization is only hypothesized by Ghiara *et al.* (1997), Ghiara *et al.* (1999) and Ghiara *et al.* (in press).

The aim of the present paper is to illustrate some distributive and textural aspects of zeolites occurring in pyroclastic flows and related rocks, to constrain minerogenetic modelling. This paper describes the ash and pumice pyroclastic flows and related rocks outcropping in a sector of northern Sardinia.

Lithostratigraphy

The sample area, including the villages of Ozieri, Ploaghe, Ittireddu, Chilivani, Mores and Bonorva (fig. 1), covering about 1000 km^2, is part of a larger one in which ignimbritic deposits, belonging to the ancient Tertiary activity, outcrop. Volcanic piles, formed of overlapping cooling units, are 70 to 300 metres thick. Minor Plio-Quaternary basaltic volcanics and continental to lacustrine Quaternary sediments also outcrop; sediments related to the Burdigalian-Serravallian marine ingression only outcrop in the western sector (near Mores). Tertiary volcanics include ash and pumice pyroclastic flows and minor pyroclastic fall deposits; epiclastic and base surge deposits are locally interbedded with pyroclastic flows.

The pyroclastic flows may be subdivided into the following two main ignimbritic groups: welded, and poorly welded. The latter show variable degrees of alteration, mainly forming zeolitic aggregates. They will therefore be the main object of this study.

The ignimbrites were mostly emplaced in subaerial environments and are found, as wide plateaux often consisting of several overlapping cooling units emplaced over a short period of time, or as thick flows in structural troughs.

As the volcanic sequences, constituted of rhyolitic to dacitic lithotypes, are dismembered by synvolcanic Oligo-Miocene up to Plio-Quaternary tectonic phases (Lecca *et al.*, 1997), a general and comprehensive stratigraphic succession representative for the whole area is not easily to reconstruct. For these reasons, and to investigate better both zeolitization processes and their areal distribution, we propose several stratigraphic columns, representative of different sectors of the study area.

These are:

Monte Mainas

The volcanic succession of Monte Mainas, about 100 m thick, resting unconformably on the Palaeozoic basement (BC), is made up, from bottom to top (fig. 2), of the following units:

– early, densely welded ignimbrites (IS);
– reddish ash and pumice flows (IC);

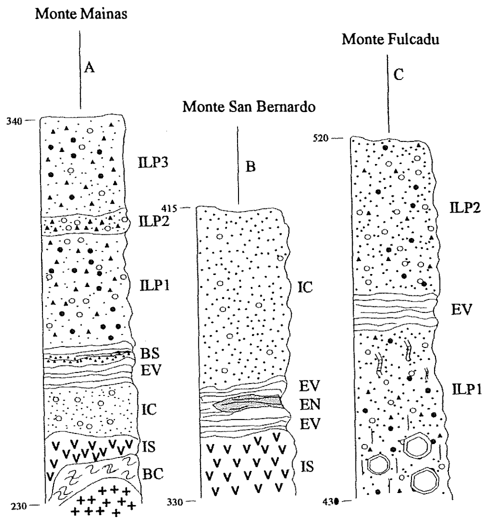

Fig. 2 – Representative stratigraphy of Oligo-Miocene volcanic sequences, including sedimentary units, from Monte Mainas, Monte S. Bernardo and Monte Fulcadu. Elevation in metres; for locations, see fig. 1*b*; for abbreviations see the text.

= gas pipe;

= reddish, silicized portion (see also Photo 3).

Photo 1 – Stratified, discontinuous levels of greenish epiclastic deposits (EV) from Monte Mainas suite.

Photo 2 – Thin, discontinuous levels of base surge deposits (BS) from Monte Mainas suite.

– stratified, discontinuous levels of greenish epiclastic deposits (EV; Photo 1);
– thin, discontinuous levels of surge deposits (BS; Photo 2);
– a thick sequence of poorly welded whitish ash and pumice flows enriched in lithic components interbedded with laminated levels strongly enriched in lithic components (ILP 1 to 3).

Monte S. Bernardo

The Monte S. Bernardo volcanic succession (fig. 2) is made up, from bottom to top, of:
– a thick, flat layer of strongly welded reddish ignimbrite (IS);
– stratified greenish epiclastic deposits (EV) of a lacustrine environment locally interbedded with blackish lenses (EN);
– a thick sequence of poorly welded, whitish ash and pumice flows (IC).

Monte Fulcadu

The volcanic pile (fig. 2), from bottom to top, is the following:
– thick sequences of poorly welded ash and pumice flows with abundant degassing pipes, locally grading to reddish, silicized facies (ILP1; Photo 3);
– thin, discontinuous levels of greenish epiclastic deposits (EV);
– thick sequences of poorly welded, whitish ash and pumice flows (ILP2).

Sant'Antonio di Bisarcio

This volcanic succession (fig. 3), with thickness decreasing eastward, is made up, from bottom to top, of the following units:
– reddish, strongly welded ignimbrites (IS);
– whitish ash and pumice pyroclastic flow deposits (IC) interbedded in their upper part with thin levels of epiclastites (EV);

Photo 3 – Monte Fulcadu suite: thick sequence of poorly welded ash and pumice flows (ILP). Degassing pipes locally grade to reddish, silicized facies.

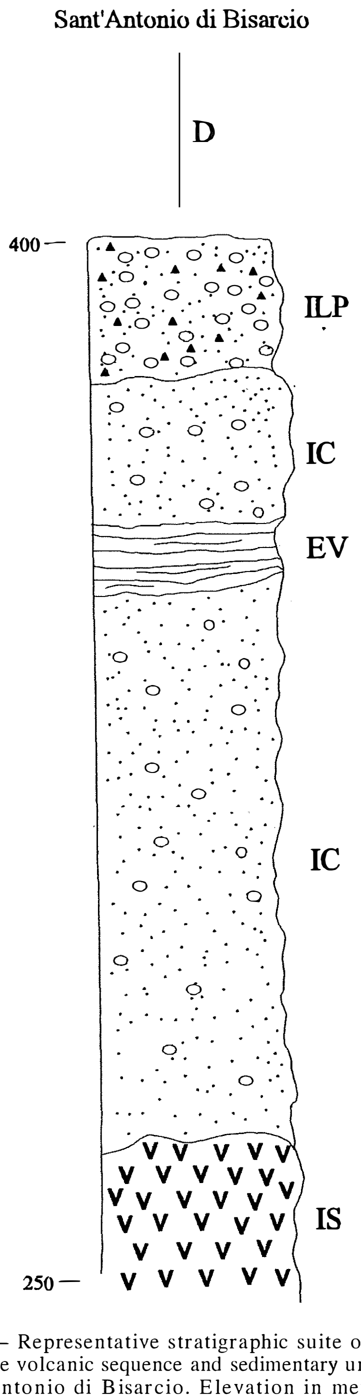

Fig. 3 – Representative stratigraphic suite of Oligo-Miocene volcanic sequence and sedimentary units from Sant'Antonio di Bisarcio. Elevation in metres; for locations, see fig. 1*b*; for abbreviations see the text.

– poorly welded whitish ash and pumice flows, enriched in lithic components (ILP).

Bonorva area

This area contains a pile, 150 m thick, of flat, overlapping, poorly welded whitish ash and pumice ignimbrites, enriched in lithic components (ILP) and emplaced over a short period of time.

To highlight both single cooling units and lateral volcanological and petrographic variations, five stratigraphic sections from different localities (fig. 4) were sampled in this area.

In summary, field relationships suggest that the ignimbrites outcropping throughout the investigated area may be grouped into three main lithological units, distinguishable by their peculiar volcanological and petrographic characters. The units are:

– early, densely welded ignimbrites (IS);

– intermediate, ash and pumice flows (IC);

– late, ash and pumice flows, enriched in coarse pumice and lithic fragments (ILP).

PETROGRAPHIC FEATURES

Pyroclastic flows

The IC ignimbrites are dominantly massive, whereas the ILP types are mostly flat and overlapping flows; the latter frequently host degassing pipes. All the pyroclastic flows are poorly sorted; stratifications are commonly lacking and vuggy fabrics exist. Locally, some ILP pyroclastic flows show internal layering, as evidenced by alternating coarse- to fine-grained layers and crude orientation of elongated pumiceous or glassy crystal plate fragments.

The random distribution of degassing pipes is apparent, although they are more abundant in the upper portions of the cooling units. The pipes (Photo 4) occur in both single and branching patterns and are depleted in dust size tephra.

Mostly in the upper parts of a single cooling unit, the ILP types grade into a reddish, silicized facies forming planar sheets or pipe-

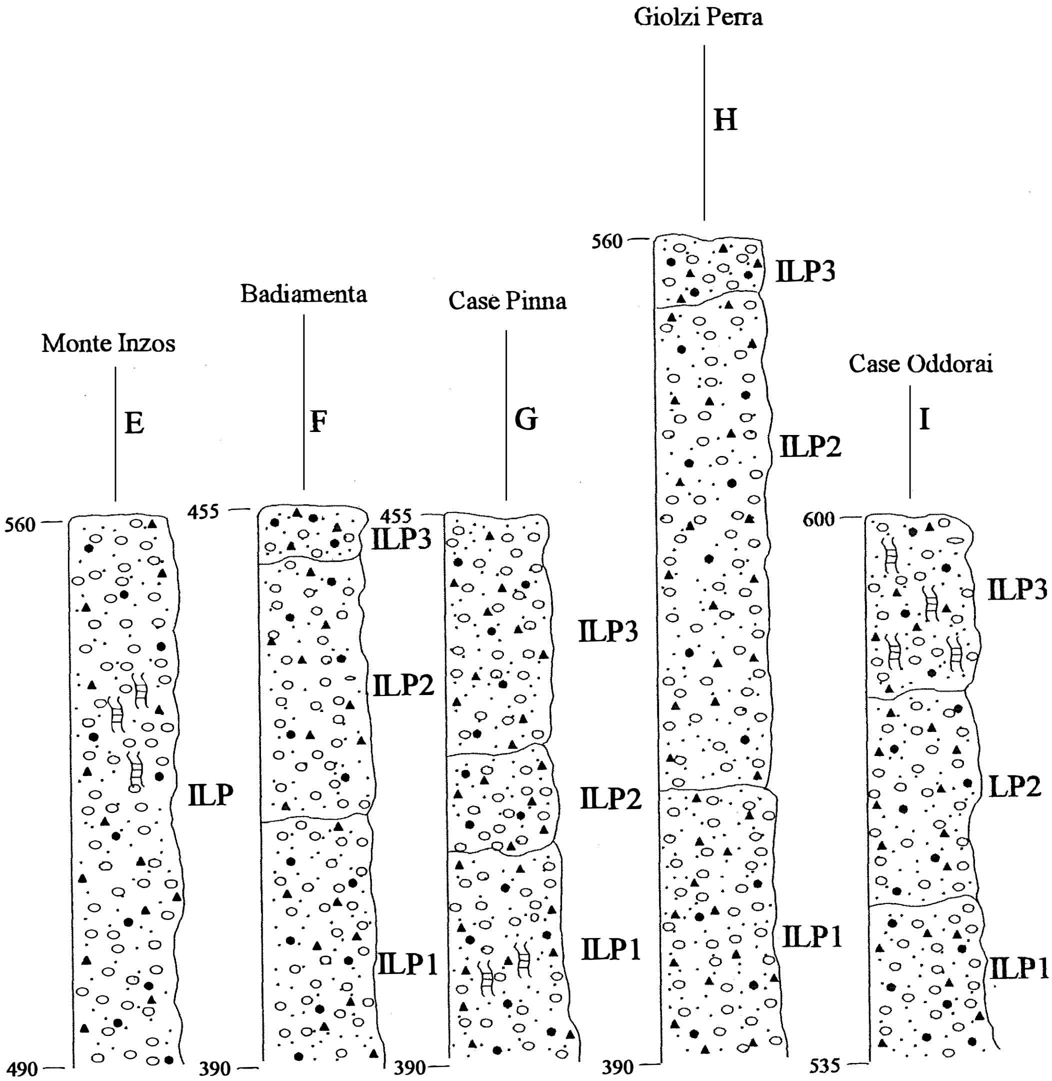

Fig. 4 – Stratigraphic suites for pyroclastic flows of Bonorva area. Elevations in metres; for location, see fig. 1*b*; for abbreviations see the text.

like circular bodies. Strongly silicized facies also occur in some IC types (cfr. sample 100 from Monte Mainas).

IC and ILP ignimbritic types differ in the following volcanological and petrographic aspects:

1) IC types are enriched in ash matrix and depleted in lithic components;

2) ILP types contain coarser pumice and glassy fragments;

3) pipes are preferentially present in the ILP types;

4) the porphyritic index ranges from 10 to 15 vol% in the IC and from 20 to 30 vol % in the ILP ignimbrites.

All the ash and pumice flows show eutaxitic

Photo 4 – Large (about 8 m high) degassing pipe structures in Bonorva area.

textures and nearly homogeneous petrographic features. Their phenocrystic association is represented, with decreasing abundance, by: zoned plagioclase, quartz, biotite, rare K-feldspar and Ca-rich pyroxene; amphibole is sporadic. Common accessory phases are Ti-magnetite, microphenocrysts and needle-like apatite crystals. Glassy grains, representing the so-called bubblewall shards, range in shape from cuspate or lunate to thin plate fragments.

Thin-section observations show that the distinctive character of the reddish silicized facies is the presence of patches and/or veins mainly filled with fine-grained aggregates of silica minerals (e.g. opaline and/or chalcedony) and zeolite. A snowflake texture develops in some strongly silicized facies of IC-type ignimbrites (e.g. samples from Monte Mainas).

Juvenile vesiculate fragments are more or

TABLE 1

Modal analyses of representative samples from Monte Inzos (MI), Badiamenta (BA), Case Pinna (CP), Giolzi Perra (GP) and Case Oddorai (CO) sectors of Bonorva area. Every data set derives from around 15,000 counted points. Samples from different sectors are listed from top to bottom. M=matrix, including cineritic and larger (>1/16 mm) glassy fragments (shards), partially transformed into minute zeolitic aggregates; Pl=plagioclase; Qz=quartz; Kf=K-feldspar+adularia; Px=pyroxene; Bt=biotite; Pm=pumiceous fragments often containing zeolite; Xand=andesitoid xenolith; Xign=ignimbritic xenolith; Xbas=Palaeozoic basement xenolith.

Sample	Altitude (m)	M	Pl	Qz	Kf	Px	Bt	Pm	Xand	Xign	Xbas
MI 2.6	558	59.7	14.5	7.7	1.9	1.5	2.0	7.4	2.7	0.8	1.3
MI 2.5	528	49.5	14.6	9.8	4.1	0.6	2.8	11.5	1.4	4.8	1.1
MI 2.4	545	45.2	9.2	10.6	3.2	0.3	2.6	22.7	2.6	2.1	1.4
MI 2.3	512	52.0	12.0	6.3	8.0	-	1.5	17.4	7.0	2.7	2.6
MI 2.2	498	40.9	10.4	7.9	5.0	-	2.8	12.5	1.9	17.8	0.7
MI 2.1	495	55.8	9.0	6.5	4.4	-	2.6	16.1	1.7	3.3	0.7
BA 3	452	41.5	11.9	9.3	5.3	-	2.8	16.3	2.2	7.0	0.3
BA 2.3	449	50.9	13.1	10.4	5.9	-	3.1	5.3	3.1	5.7	1.0
BA 2.2	434	45.7	19.3	10.9	5.4	-	4.7	3.2	4.5	5.6	0.8
BA 2.1	422	44.0	18.0	6.5	5.2	-	2.9	12.9	4.1	5.2	1.0
BA 1.3	416	44.7	22.6	13.4	4.6	0.4	3.9	3.0	2.6	3.3	1.5
BA 1.2	408	45.3	13.6	16.5	6.0	0.2	3.4	11.1	1.2	1.5	1.1
BA 1.1	398	42.3	21.6	11.4	6.2	-	2.8	8.4	2.9	3.6	0.8
CP 3.4	450	39.2	14.6	11.1	2.2	-	8.6	5.6	7.0	2.5	2.1
CP 3.3	439	31.0	18.8	17.0	2.2	1.0	10.4	8.7	1.7	7.6	1.6
CP 3.2	433	49.1	11.3	10.9	3.2	-	7.7	8.6	3.0	4.2	1.9
CP 3.1	427	7.9	20.7	17.9	2.5	-	10.5	28.4	2.0	1.1	2.9
CP 2.3	422	29.8	15.8	13.7	3.0	0.7	17.2	13.7	2.5	0.6	2.5
CP 2.2	416	27.7	15.0	12.2	1.9	-	13.5	14.4	3.5	10.7	0.2
CP 2.1	412	26.3	20.2	11.0	2.6	-	11.8	20.1	4.3	1.0	1.7
CP 1.4	407	38.9	16.6	12.3	2.8	-	7.9	11.9	2.6	4.5	2.2
CP 1.3	401	49.0	13.9	15.5	2.4	-	4.1	8.1	3.4	1.3	2.3
CP 1.2	395	52.7	16.6	7.2	3.3	-	3.3	9.9	3.3	2.6	1.0
CP 1.1	391	42.8	13.3	17.2	2.8	-	5.7	12.3	3.2	1.1	1.6
GP 3	592	50.7	6.5	12.1	0.4	-	1.6	16.1	4.0	4.5	0.9
GP 2.4	585	45.8	9.4	12.2	0.6	-	3.5	16.1	4.0	4.5	0.9
GP 2.3	555	29.0	15.0	30.3	1.2	-	2.9	11.6	1.7	3.4	2.7
GP 2.2	545	46.3	11.6	20.7	1.1	-	1.9	3.4	4.5	2.9	2.3
GP 2.1	520	29.7	18.2	17.5	1.0	-	3.5	18.7	3.2	1.9	2.2
GP 1.2	509	55.3	10.2	10.8	0.8	-	3.3	11.9	1.6	4.5	1.6
GP 1.1	498	65.3	11.7	9.5	0.2	0.1	2.4	4.3	1.3	3.9	1.1
CO 3.3	598	70.5	15.6	2.1	0.5	-	1.6	7.8	0.6	0.9	0.3
CO 3.2	593	70.3	12.3	5.2	0.7	0.1	1.7	6.0	1.8	1.1	0.5
CO 3.1	579	62.7	9.7	4.7	0.7	0.8	1.5	18.2	0.1	1.1	0.3
CO 2.3	572	56.1	10.9	6.7	0.9	0.3	1.9	16.8	1.4	3.8	1.2
CO 2.2	567	56.5	10.8	1.4	0.3	-	1.8	23.9	1.3	4.0	-
CO 2.1	559	55.1	15.6	4.4	0.5	-	1.7	14.6	3.0	3.0	1.6
CO 1.2	550	45.3	21.6	9.2	2.0	2.0	3.7	8.7	0.3	3.9	3.4
CO 1.1	539	41.0	15.4	6.9	1.3	-	1.9	24.2	1.5	6.7	0.3

less flattened and stretched, with typical flame terminations.

Two end-member types of vesicules (Fisher and Schmincke, 1984) were identified: tubular, and spherical to sub-spherical varieties. The former are characteristic of elongated fibrous pumices; the latter, particularly frequent in the IC ignimbrites, are mainly found in the central portions of fibrous and rounded pumices.

Lithic components are represented by angular to subrounded fragments of andesites, welded ignimbrites, and Palaeozoic crystalline basement.

Modal analyses of representative samples from various sectors of the Bonorva area were carried out; analytical data are listed in Table 1. In this table, sporadic magnetite, constantly represented by minute grains, is omitted.

Matrix (M) and pumiceous fragments (Pm) include zeolitic minerals; plagioclase, quartz, K-feldspar, pyroxene and biotite are representative of phenocryst assemblages.

Vertical variations, excluding the lithic components (xenoliths) for the various sectors, are shown in fig. 5.

The matrix, with the exception of sample CP 3.1, is always the most abundant fraction in the samples, and plagioclase is the most representative mineral among the phenocryst assemblage, where pyroxene is always only sporadic. Fig. 5 clearly shows a negative correlation between crystal-glassy ash and pumiceous fragments.

Almost all ash and pumice flows underwent more or less post-depositional transformation processes; in addition, several ignimbrites were percolated by late, silica-rich fluids.

Secondary minerals, as revealed by thin section, X-ray and electron microscope analyses, with decreasing abundance, are:

– zeolite;
– smectite;
– silica minerals (opal-CT, chalcedony);
– K-feldspar (adularia);
– calcite and glauconite only occur in the surge and greenish epiclastic deposits.

Qualitative results from X-ray powder diffraction analyses of representative samples are listed in Table 2.

Clinoptilolite is the most abundant zeolite variety, followed by mordenite. Sporadic analcime grains were only observed in a few samples from Sant'Antonio di Bisarcio pyroclastic flows.

Pyroclastic surges

Surges occur in the volcanic piles as centimetric and decimetric discontinuous levels. They are poorly sorted and show bedding structures such as planar beds, low-angle cross-stratifications and dune forms. Their porphyritic indexes range from 35 to 50 vol% in the coarse-grained lithic- and crystal-rich levels and from 5 to 10 vol% in the fine-grained ash-cloud deposits. Thin layers enriched in juvenile vesiculated fragments also occur.

The phenocryst components are mainly represented by plagioclase (An_{55-25}) clasts, embayed quartz and biotite laths; rare pyroxene grains may also be observed. The lithic component is very similar to that of the pyroclastic flows. The crystal-glassy matrix is more or less abundant, and perlitic cracks are frequent in the glassy component.

The matrix is locally affected by post-depositional alteration processes, with the formation of patches of felt-form aggregates of tabular, well-developed clinoptilolite crystals. In addition, late veins filled by early clinoptilolite and late calcite aggregates are sometimes observed.

Epiclastic deposits

Epiclastites occur in the pyroclastic suites as more or less thin, greenish or blackish levels, characterized by low-angle and planar lamination, with coarse tail grading; they are occasionally massive. Coarse, denser clasts range from 25 vol% (upper portion) to 40 vol% (lower portion).

Like the related pyroclastic deposits, the crystalline component is represented by plagioclase grains (An_{60-30}), rounded quartz

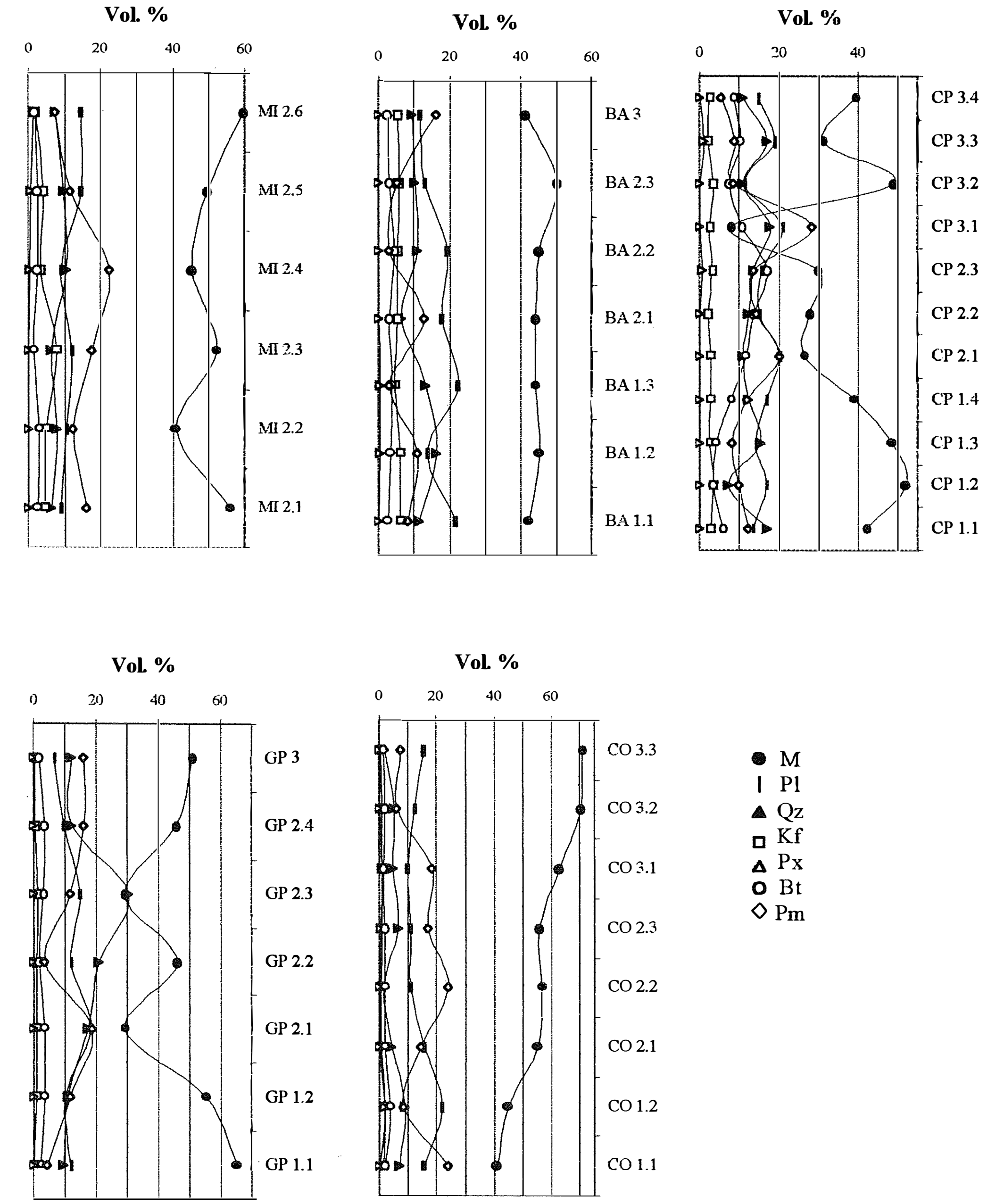

Fig. 5 – Vertical variations in modal contents for the samples listed in Table 1. MI=Monte Inzos; BA=Badiamenta; CP=Case Pinna; GP=Giolzi Perra; CO=Case Oddorai; M= matrix; Pl=plagioclase; Qz=quartz; Kf=K-feldspar+adularia; Px=pyroxene; Bt=biotite; Pm=pumice. Xenolithic components are omitted.

TABLE 2

*X-ray qualitative analyses for representative samples from various stratigraphic suites. Pl=plagioclase; Qz=quartz; Kf=K-feldspar+adularia; Sm=smectite; Bt=biotite; Px=pyroxene; Mt=magnetite; Clino=clinoptilolite; Opal=opal-CT; - =below detection limit; *=sporadic; **=scarce; ***=frequent; ****=abundant; gp=gas pipe. Samples are listed according to their stratigraphical position.*

Sample	Pl	Qz	Kf	Sm	Bt	Px	Mt	Clino	Opal
				Monte Mainas					
124	****	**	*	*	*	-	*	*	-
141.2	***	***	*	*	**	-	*	***	-
141.1	***	**	*	*	*	-	*	**	-
132B	***	**	*	*	**	-	*	**	-
132A	***	***	*	*	*	-	*	**	-
120.3	***	**	*	*	-	-	*	**	-
120.2	***	**	*	*	**	-	*	*	-
101.4	***	***	*	*	**	*	*	***	-
101.3	***	**	*	*	**	*	*	****	-
101.2	***	**	*	*	*	-	*	**	-
101.1	***	**	*	*	*	-	*	****	-
130C	***	**	*	*	*	-	-	***	-
130B	***	**	*	*	**	-	-	***	-
130A	***	**	*	*	**	-	-	****	-
134B	***	***	**	*	**	-	-	*	-
134A	****	**	**	*	*	**	-	**	-
138.3	****	**	*	*	**	**	*	-	-
138.2E	***	**	*	*	*	*	*	****	-
138.2D	***	**	*	*	*	-	*	***	-
138.2C	***	-	*	*	**	*	*	****	-
138.2B	***	**	*	*	**	-	*	****	-
138.2A	***	**	*	*	**	-	*	****	-
138.1	**	-	*	*	**	-	*	***	-
100F	***	*	**	*	*	-	-	-	-
100E	***	*	**	*	*	-	-	-	-
100D	***	*	**	*	*	-	-	-	-
100C	***	*	**	*	*	-	-	-	-
100B	***	*	**	*	*	-	-	-	-
100A	***	*	**	*	-	-	-	*	-
137	**	**	*	*	*	*	*	***	-
91	***	-	*	*	**	-	-	**	-
94	***	-	*	*	*	*	*	***	-
				Monte San Bernardo					
240	***	**	**	*	*	-	*	*	-
581	***	**	*	**	**	-	-	**	-
582	***	**	*	*	**	-	*	****	-
				Monte Fulcadu					
205.4	***	*	*	*	*	-	*	***	***
205.3	***	-	*	*	**	*	*	***	**
204.2	**	-	**	*	**	-	-	**	-
205.1	***	-	**	*	**	*	-	***	-
205.5	****	*	**	*	*	-	-	**	-
205.0	***	*	*	*	**	-	*	****	**
214.1	***	-	*	*	**	-	*	****	**
214.2	***	-	*	*	**	-	*	***	***
214.3	****	-	**	*	**	-	*	*	-

TABLE 2: *Continued*

Sample	Pl	Qz	Kf	Sm	Bt	Px	Mt	Clino	Opal
				Sant'Antonio di Bisarcio					
202	***	*	*	*	*	-	*	**	-
201	***	*	*	*	*	-	*	*	-
200	***	**	*	*	*	-	*	**	-
191	****	*	*	*	*	*	*	*	-
184.2	***	**	*	*	*	-	*	***	-
188.2.2	**	*	*	*	*	-	*	***	**
232.2	**	**	*	*	*	-	*	*	-
188.2.1	***	*	*	*	*	-	*	***	**
232.1	****	**	*	*	*	-	*	-	-
188A	****	**	*	*	*	-	-	-	-
188.1	***	*	*	*	*	-	*	*	-
184.1	***	*	*	*	*	-	*	*	-
190	***	*	*	*	*	-	*	*	-
213	***	*	*	*	*	-	-	*	-
				Monte Inzos					
MI2.6	**	**	*	*	*	*	-	**	*
MI 2.5	**	**	**	-	**	-	*	***	*
MI 2.4gp	**	**	**	*	**	*	*	***	*
MI 2.4	**	**	**	*	**	*	*	***	*
MI 2.3	**	*	**	*	**	*	-	***	*
MI 2.2	**	*	**	*	**	*	-	***	*
MI 2.1	**	*	**	*	**	*	*	***	*
				Badiamenta					
BA 3	**	*	*	*	*	*	*	***	*
BA 2.3	**	*	*	*	**	*	*	***	*
BA 2.2	**	*	**	*	**	*	*	***	*
BA 2.1	***	**	**	*	**	*	*	**	*
BA 1.3	***	**	*	*	**	*	*	***	*
BA 1.2	**	**	**	*	**	*	*	****	*
BA 1.1	**	*	**	*	**	*	*	***	*
				Case Pinna					
CP 3.4	**	*	*	*	*	-	-	**	*
CP 3.3	**	*	*	-	**	*	-	***	*
CP 3.2	***	**	*	*	*	*	*	***	*
CP 3.1	***	**	*	*	**	-	*	***	*
CP 2.3	***	**	*	-	**	*	-	**	*
CP 2.2	***	**	*	-	**	*	-	***	*
CP 2.1	****	**	*	*	**	*	-	**	*
CP 1.4	****	**	*	-	*	*	-	**	*
CP 1.3gp	****	**	*	-	**	*	-	**	*
CP 1.3	****	***	*	*	**	*	-	***	*
CP 1.2	****	***	*	*	**	*	-	**	*
CP 1.1	****	***	*	*	**	-	-	**	*
				Giolzi Perra					
GP 3	**	*	*	*	*	*	*	***	*
GP 2.4	***	**	*	*	**	*	*	***	*
GP 2.3	**	**	*	*	**	*	-	****	*
GP 2.2	***	**	*	*	*	*	*	***	*
GP 2.1	***	**	*	*	*	*	*	**	*
GP 1.2	***	**	*	-	*	*	-	***	*
GP 1.1	***	**	*	*	*	*	*	**	*
				Case Oddorai					
CO 3.3	***	*	*	*	*	*	*	*	*
CO 3.2gp	**	*	*	-	*	-	-	**	*
CO 3.2	**	*	*	*	**	*	*	***	*
CO 3.1gp	**	*	*	*	**	*	*	**	*
CO 3.1	***	*	*	*	**	-	-	****	*
CO 2.3	***	*	*	-	*	-	*	***	*
CO 2.2	**	*	*	-	**	-	-	****	*
CO 2.1	**	*	*	-	**	*	*	***	*
CO 1.2	**	**	*	*	**	-	*	****	*
CO 1.1	***	*	*	-	*	*	*	**	*

and biotite laths. Very rare pyroxene grains are also observed. The angular to sub-rounded lithic component is made up of welded and poorly welded ignimbrites, andesites and crystalline basement clasts.

The crystal-glassy matrix frequently shows evidence of alteration processes, consisting of newly formed zeolite and minor clay minerals growing in the interstitial patches and/or on the crystalline component. Rare veins filled with zeolitic and calcitic aggregates are also observed; they show peculiar zoning, consisting of felt-form aggregates of well-shaped, tabular clinoptilolite crystals and, filling the central part, anhedral calcite aggregates.

Distribution and crystallization sequence of secondary minerals

X-ray diffraction patterns (Table 2) and thermal analyses (not reported) indicate that the amounts of secondary minerals are very variable, both within the volcanic sequences and inside a single cooling unit (Morbidelli, 1999).

Quantitative variations in zeolite and other main secondary minerals, desumed from X-ray R.I.R. (Reference Intensity Ratio) analyses

TABLE 3

*Secondary mineral variation range (wt%) in various lithotypes as desumed from Rietveld-RIR analyses. IC= ash and pumice flows; ILP= ash and pumice flows enriched in lithic component; BS=base surge deposits; EV=epiclastic deposits. Sm=smectite; Clino=clinoptilolite; Mord=mordenite; Ana=analcime; Opal= opal-CT; Glauc=glauconite; - =below detection limit; *=rare.*

Type	Sm %	Clino %	Mord %	Ana %	Opal %	Glauc %
IC	1-5	6-43	-	-	4-5	-
ILP	0-4	0-53	7-9	*	0-6	-
BS	2-3	53-35	-	-	0-7	-
EV	1-2	17-21	-	-	-	*

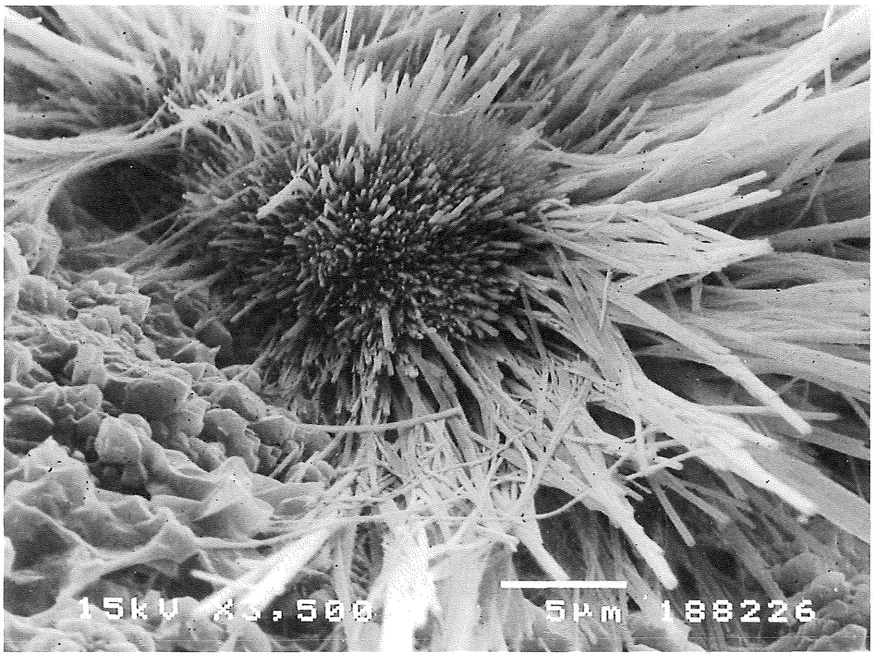

Photo 5 – Mordenite radiating crystalline aggregates in vugs; scanning electron micrograph, Sant'Antonio di Bisarcio, sample 188.2.2.

(Morbidelli, 1999) on representative samples, are listed in Table 3.

On the whole, the data are in good agreement with the results obtained by Ghiara *et al.* (1997) and Langella *et al.* (1999) on pyroclastic and tuffitic rocks from northern Sardinia. However, close comparison between the three data-sets reveals that on average, zeolite contents in the samples investigated by Ghiara *et al.* (1997) and Langella *et al.* (1999) are higher.

Radiating clusters of thin, fibrous mordenite crystals in close association with opal-CT lepispheres, occurring in vugs, are widespread (Photo 5). Only in the Sant'Antonio di Bisarcio pyroclastic flows do trapezoidal high-silica analcime grains (Si/Al ≅2.6) and fibrous mordenite coexist. Euhedral, tabular clinoptilolite crystals are also frequently found in the vugs of pyroclastic flows from the Bonorva area; in the last occurrence, opal-CT lepispheres (Photo 6) and occasional late mordenite fibres grow on euhedral clinoptilolite grains.

Tubular (Photo 7*a*-*b*) and sub-spherical (Photo 8*a*-*b*) vesicles inside pumiceous fragments are partially filled with radiating, euhedral clinoptilolite crystals and/or opal-CT lepispheres. Glass rinds may be smooth or scattered with micropits generating a bubble-wall texture (Fischer, 1963). It is interesting to note that the thin glassy border remains unaltered as clearly shown by microprobe analyses (Morbidelli, 1999).

Clinoptilolite growing on cuspate, lobate and platy shards display euhedral terminations towards the central portion of the fragments (Photo 9*a*-*b*). In several occurrences, clinoptilolite crystals grow on thin films of early smectitic lamellae. Radiating mordenite fibres growing on the glassy fragments occur rarely. Newly formed adularia on the external rind of shard fragments occurs in strongly silicized rocks (e.g. sample 100 from Monte

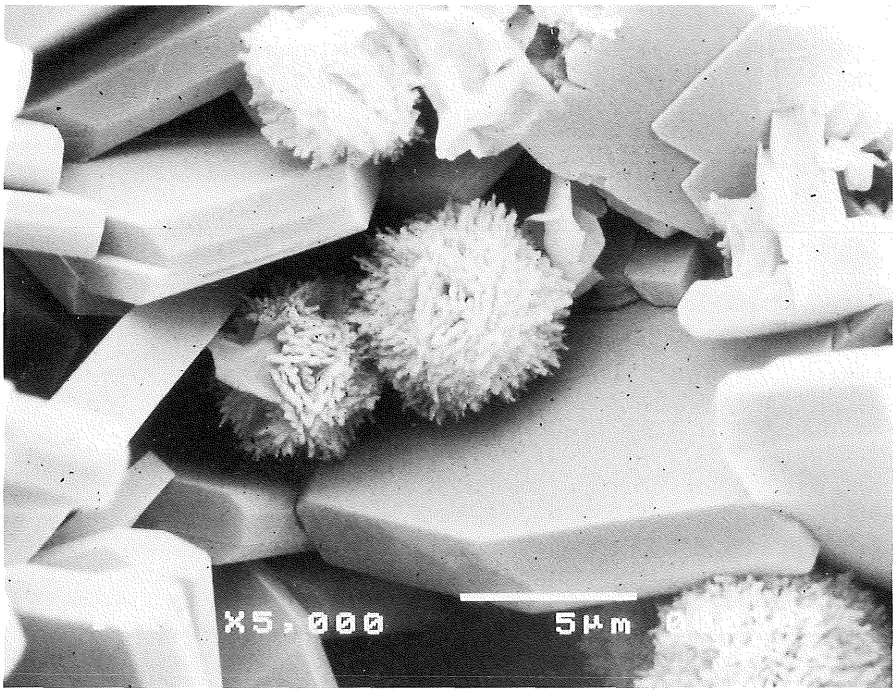

Photo 6 – Scanning electron micrograph of intergrown tabular clinoptilolite crystals associated with later opal-CT lepispheres in vugs from IC pyroclastic flows outcropping near Case Oddorai.

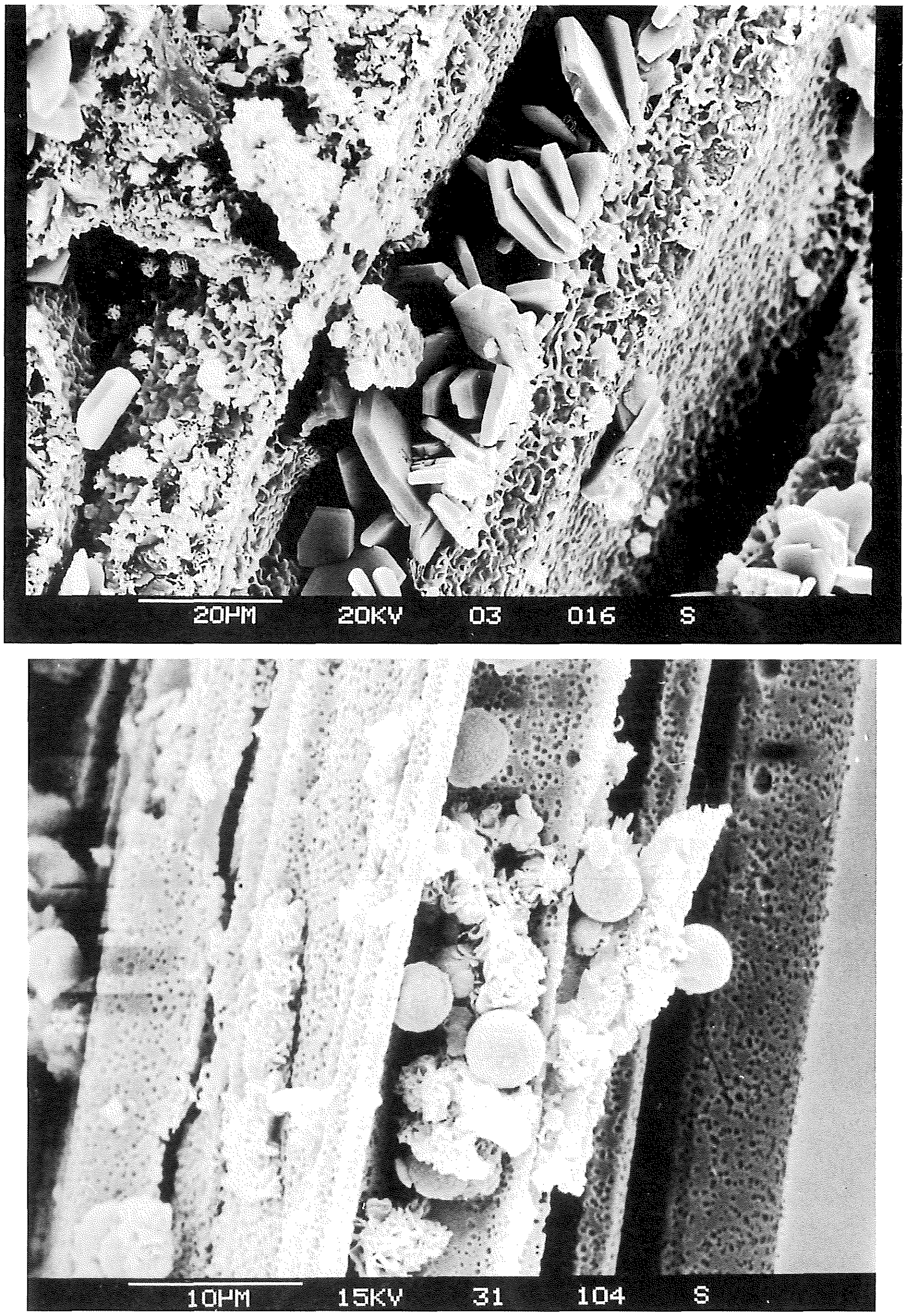

a

b

Photo 7 – *a*) Scanning electron micrograph of tubular vesicles inside pumiceous fragments from Monte Mainas ignimbrites (ILP) lined with euhedral clinoptilolite crystals and *b*) opal-CT lepispheres. Note scattered micro-pits resulting from high degree of vesiculation of glass.

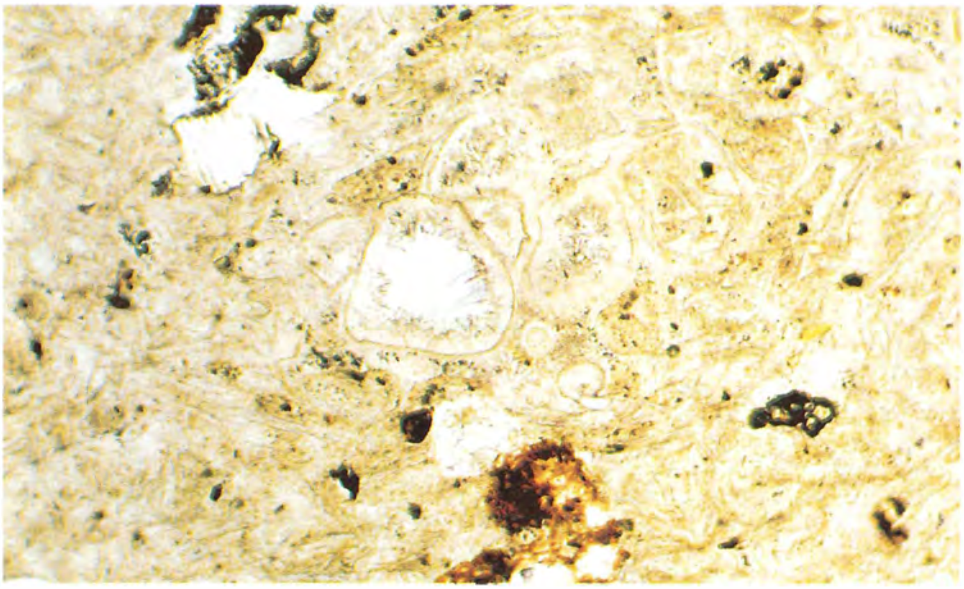

a

b

Photo 8 – Sub-spherical vesicles. *a*) Cluster of sub-spherical vesicles from disaggregated juvenile vesiculated fragments in matrix from pyroclastic flows of Monte Mainas, sample 138.2, plane polarized, 150 × *b*) Detail from scanning electron microscopy, broken sub-spherical vesicle lined with radiating, euhedral clinoptilolite crystals growing inside.

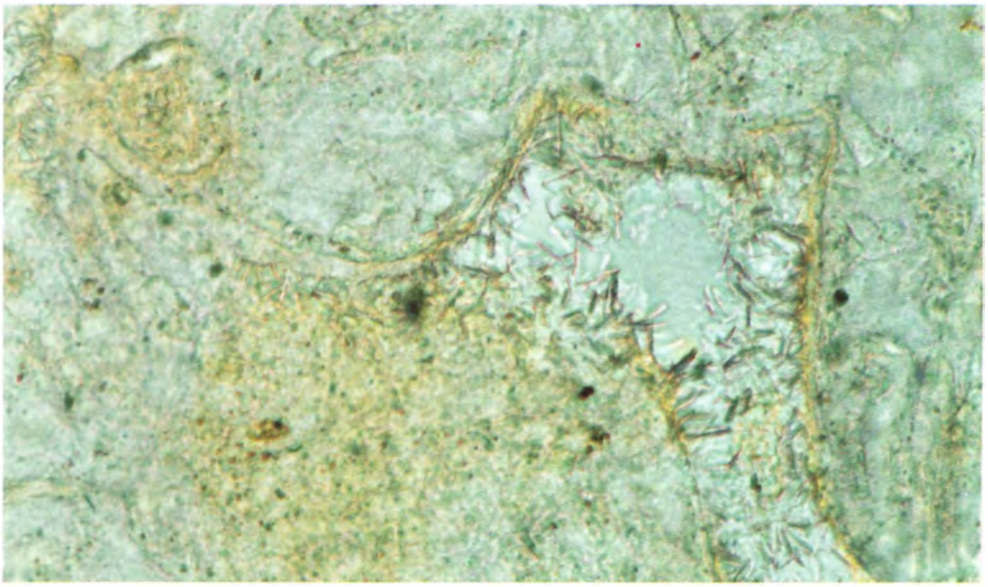

a

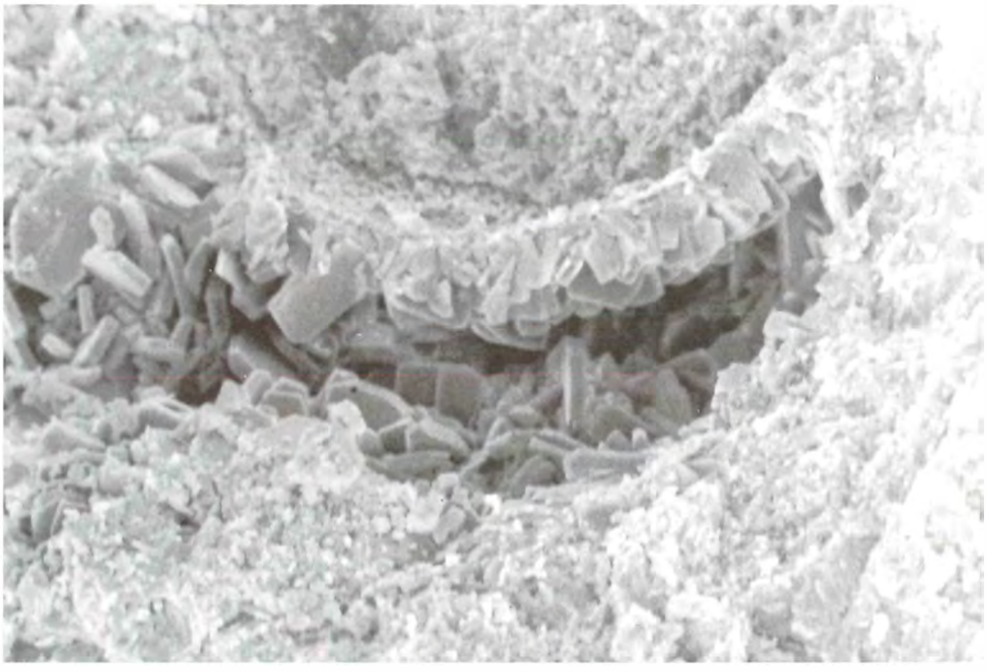

b

Photo 9 – *a*) Cuspate shards partially transformed into clinoptilolite aggregate of Giolzi Perra ignimbrites, plane polarized 250×, *b*) Detail from scanning electron microscopy, 500×, of a cuspate shard: note clear cut euhedral terminations towards central portion of clinoptilolite crystals.

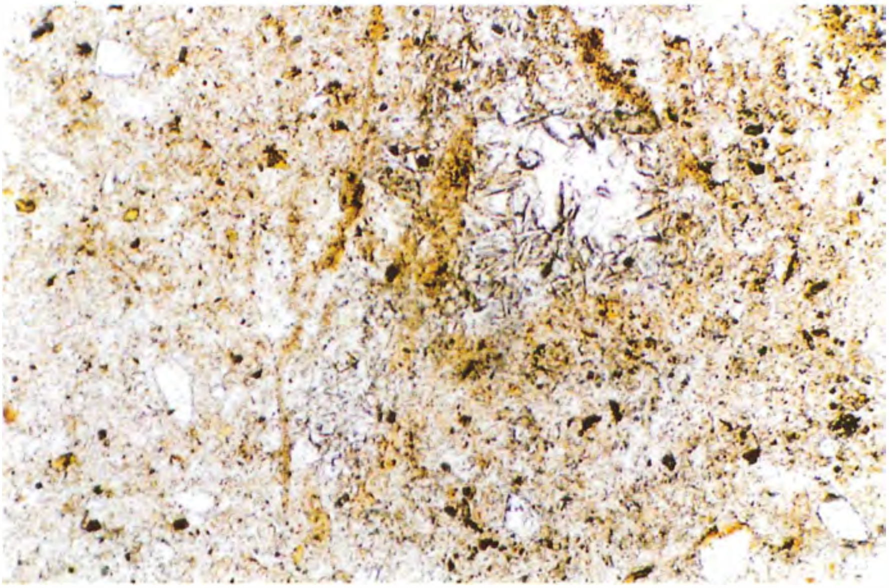

a

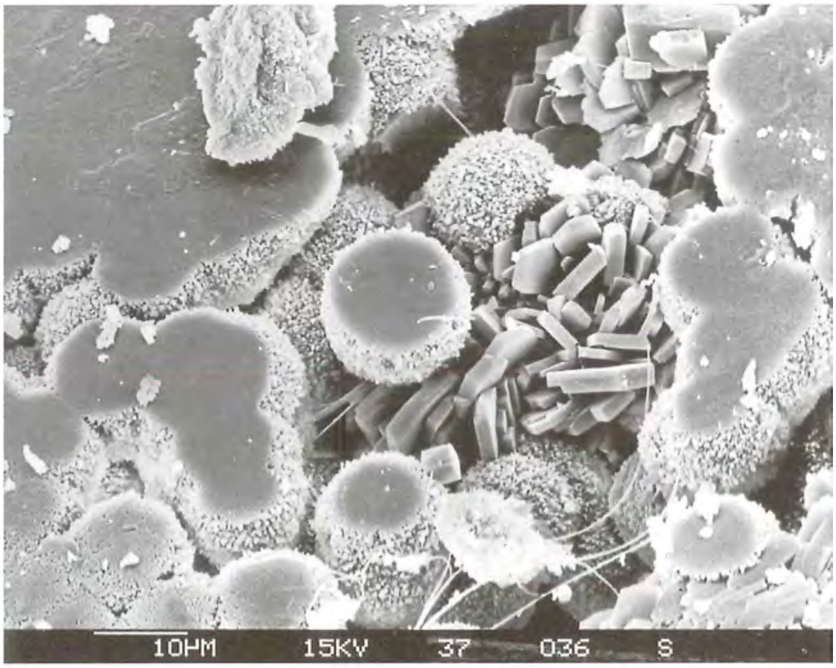

b

Photo 10 – *a*) Patches of silicized regions in pyroclastic flows from Monte Mainas, sample 100A. Plane polarized 100×, *b*) Detail from scanning electron microscopy of silicized region showing abundant opal-CT lepispheres growing on tabular clinoptilolite crystals. Note (bottom) rare late fibres of mordenite.

Mainas); it should be noted that zeolitic minerals are nearly always lacking in this rock-type.

Patches, distributed on the matrix and showing intergrowths of silica minerals and clinoptilolite are mostly widespread in the silicized facies. In these occurrences, aggregates are dominated by silica minerals; clinoptilolite is clearly an early phase (Photo 10 *a-b*), whereas rare mordenite fibres represent the last one. In strongly silicized rock types (e.g. sample 100 from Monte Mainas), zeolitic minerals are lacking.

Felt-form patches consisting of well-developed clinoptilolite crystals only occur in the base surge and epiclastic deposits (Photo 11). It is interesting to see that the zeolitized patches grade towards unaltered regions of the glassy matrix.

Rare veins (Photo 12*a-b*), lined with euhedrally terminated clinoptilolite crystals set in a calcitic matrix, only occur in epiclastic and base surge deposits (Photo 12*b*).

In summary, the above overall microscopic (optical and SEM) data set, for zeolite and other secondary minerals, show that they are distributed as follows:

1) filling vugs and degassing pipe structures;

2) lining both tubular and sub-spherical vesicles in pumices;

3) growing on cuspate glassy fragments;

4) intergrowing with silica minerals in patches randomly distributed in the matrix;

5) felt-form intergrowths of well-developed clinoptilolite crystals growing on the matrix;

6) lining veins which, in the central part, are filled with anhedral calcitic aggregates.

Textural relationships broadly indicate the following crystallization sequence for the more widespread authigenic minerals:

smectite ⇒ clinoptilolite ⇒ opal-CT ⇒ mordenite

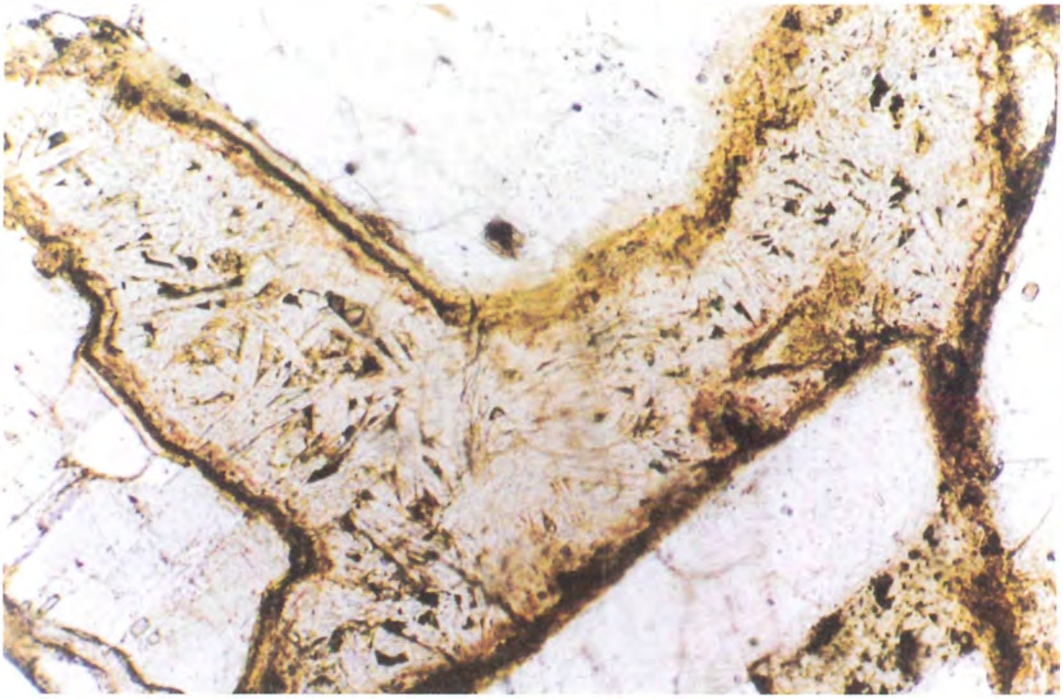

Photo 11 – Epiclastic levels. Clastic grains in patches consisting of felt-form aggregates made up of well-developed clinoptilolite crystals. Plane polarized 40×; Monte Mainas, sample 138.3.

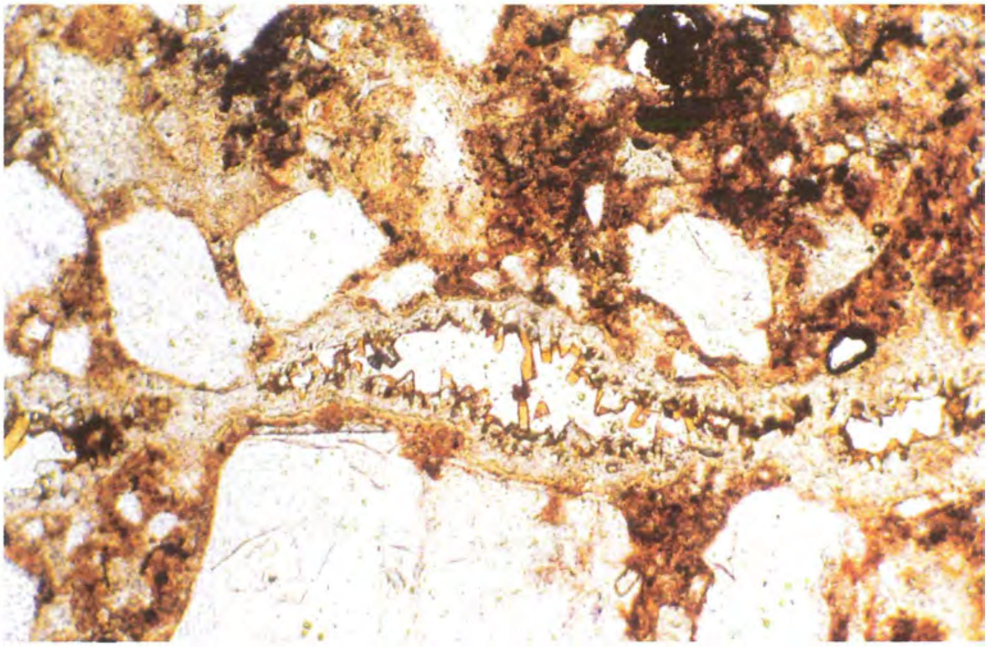

a

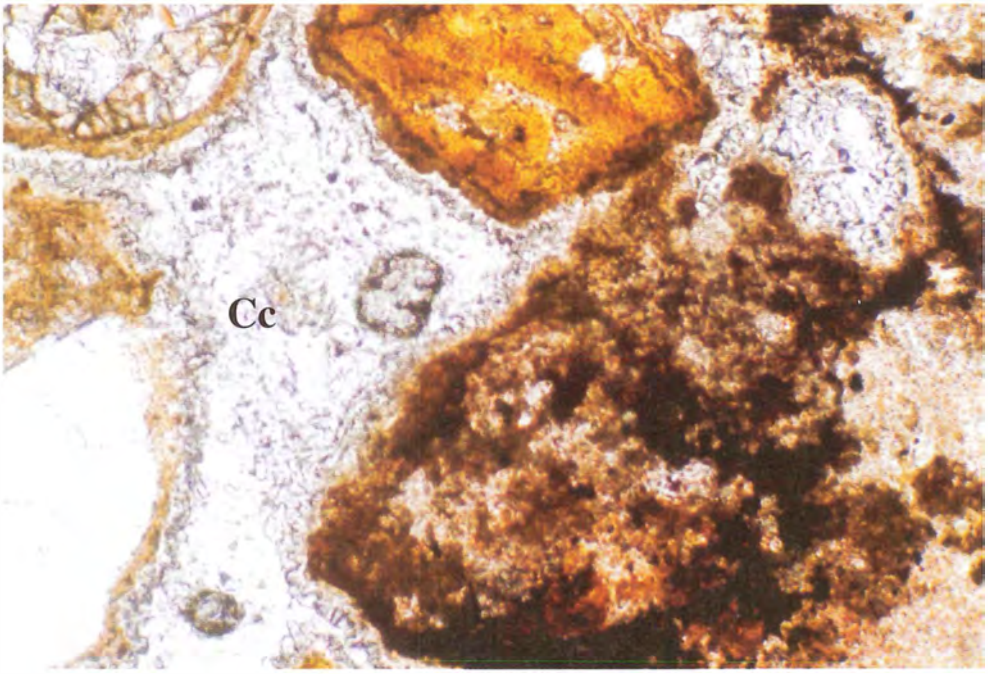

b

Photo 12 – *a*) Vein lined with radiating euhedrally terminated clinoptilolite crystals growing towards central parts sometimes *b*) showing abundant calcite crystallization. Plane polarized, 20×; Monte S. Bernardo, sample 58A; Cc = calcite.

Moreover, rare high-silica analcime grains in some vugs of pyroclastic rocks from Sant'Antonio di Bisarcio crystallized after mordenite fibres. Significantly, in the latter pyroclastic flows, hydrothermal analcime filling lithoclase also occurs.

Discussion

Minerogenetic modelling for zeolite occurring in Tertiary pyroclastic and related rocks of northern Sardinia is constrained by several volcanological, distributive and textural aspects.

Clinoptilolite growing inside armoured sub-spherical vesicles hosted in pumiceous fragments must be related to crystallization from entrapped fluids. This is in good agreement with several aspects including:

1) euhedral forms, projecting into the inner regions of vesicles, typical of freely growing crystals;

2) close paragenetic association with silica minerals, mainly represented by opal-CT lepispheres, which are typically late phases in rhyolitic ignimbrites world-wide;

3) lack of evidence concerning glassy rind transformation processes, which are in turn almost always required to form zeolitic aggregates.

All these considerations support the hypothesis that the clinoptilolite lining tubular and sub-spherical vesicles may be considered as the crystallization products from entrapped fluids.

Significantly, sub-spherical vesicles, typical of high vapour pressure during eruptions (Ewart, 1963), are enriched in clinoptilolite with respect to tubular ones which, instead, indicate lower pressure regimes.

Vugs lined with late and euhedral crystals are commonly thought to be collection spaces for exsolved silica and alkali-rich fluids, as evidenced by related crystallized phases (cfr. tridimite, adularia) and/or gas. Zeolite growing inside vugs, therefore, may be related to fluids which, during their migration through different portions of the deposits, precipitated late minerals mainly inside pore spaces.

Evidence of percolating silica and alkali-rich cooling fluids and of circulating vapours are:

– widespread and, locally, severe fumarole activity;

– the presence of late silicized patches on a microscopic scale giving ignimbrites a spotted appearance;

– veins, locally forming wider patches, mainly filled by silica minerals (Photo 13).

It is important to recall that the silicized facies of cooling units are easily recognizable in the field, owing to their reddish colour and greater coherence.

The zeolitic aggregates of the vugs fall into two main types dominated by: *a*) mordenite and opal-CT, and *b*) clinoptilolite and opal-CT with minor mordenite. This is due to differences in some intensive variables of the fluids such as crystallization temperatures, silica contents and K/Na ratios (Wirsching, 1976; Alexiev and Djourova, 1988; Barth-Wirsching and Holler, 1989; Münch *et al.*, 1996)

Moreover, crystallization sequences (e.g., opal-CT after clinoptilolite; minor mordenite fibres after opal-CT) indicate chemical systems evolving towards Na- and silica-rich compositions.

In summary, zeolitic aggregates lining vugs are probably related to crystallization from fluids of different compositions.

Clinoptilolite growing on shards requires a different minerogenetic model, involving initial glass dissolution, followed by crystallization of secondary phases in the newly-formed pore spaces. This is imposed by both crystallization sequences and the euhedral terminations of clinoptilolite. Simple devetrification cannot account for the lack of typical devetrification textures such as fibrous spherulite, axilite, and bow-tie and granophyric aggregates (Lofgren, 1970; 1971a; 1971b).

The widely investigated transformation of silicic glass by interacting fluids (Potter and Dickson, 1980; Hawkins, 1981; Wirsching, 1981; Ghiara *et al.*, 1993; Ghiara and Petti, 1996) is considered a polyphase process: an

Photo 13 – IC ignimbrites. Note the vein filled by silica minerals revealing presence of silica-rich circulating fluids. Monte Mainas.

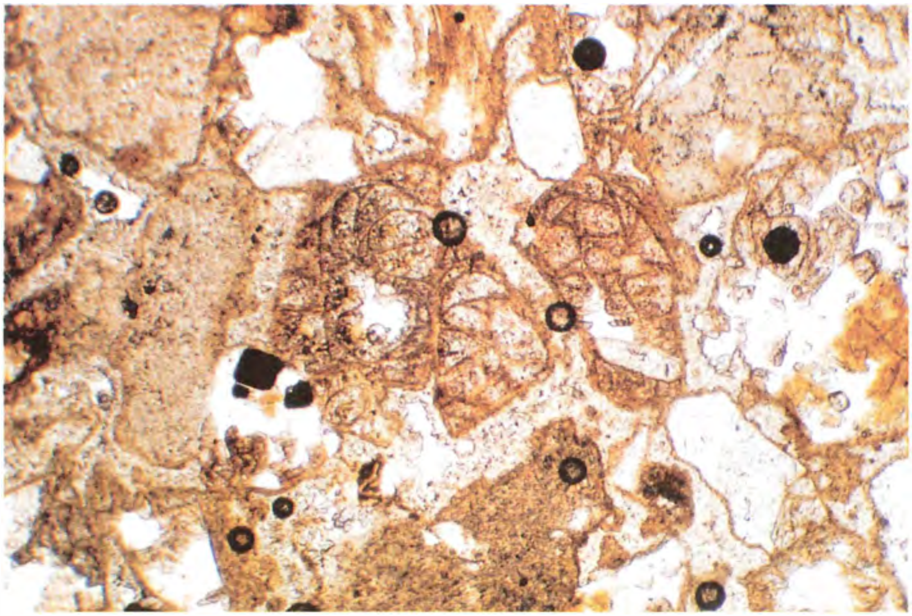

Photo 14 – Base surge levels. Perlitic structures on glassy matrix. Note interstitial clinoptilolite patches. Plane polarized, 40×; Monte Mainas, sample 130C.

initial stage dominated by diffusion and controlled hydration is followed by one of glass destruction and then secondary mineral precipitation. During the first stage, if the systems are dominated by fluids, perlitic cracks form (Photo 14); these structures are missing in both the glassy fragments and matrix of investigated ignimbrites, indicating low fluid/solid ratios during transformation processes. Moreover, in relatively closed systems, exchanges between alkali (Na^+, K^+) and hydronium ions (H_3O^+) lead to an pH increase in pore solutions. High pH values (> 9) promote both rapid dissolution of SiO_2 and zeolite crystallization. Referring to crystallization sequences of secondary minerals within clinoptilolite-bearing shards (cfr. smectite $\Rightarrow$ clinoptilolite), the small amounts of early montmorillonite must very probably be linked to a swift increase in pH, generating unfavourable conditions for smectite crystallization.

An intriguing problem is given by the variations in the alteration degrees of shards occurring even within a single cooling unit; partially to fully altered glassy fragments have been observed. Microscopic evidence indicates that the alteration process moved from shard core to rim, as emphasized by a comparison of coarse-grained cuspate shards which have undergone varying degrees of alteration. The above scenario indicates randomly variable reactivity of glass, probably due to differing thermal histories (cfr. undercooling) and/or quantities of entrapped micro-bubbles. With respect to the ILP types, the IC ignimbrites show volcanological features typical of eruptions with higher vapour pressure and magma fragmentation (cfr. spherical vesicle contents and shard/ash ratios). Significantly, the IC types generally display lower alteration of the glassy component.

Concerning minerogenetic modelling two main problems arise:

a) identification of the nature and composition of interacting fluids;

b) explanation of the variations in secondary alteration degrees, both in single and overlapping cooling units.

Several geological, volcanological and petrographic aspects indicate that juvenile fluidizing component of pyroclastic flows should be considered as the main source of interacting components.

From a petrographic point of view, it is important to recall that all the ignimbrites have phenocryst associations and chemical compositions of glassy components closely comparable. Volcanological characters (e.g. porosity, welding, sorting) are also very similar.

As regard geological features, most Tertiary ignimbrites outcropping in the investigated area were mainly emplaced in a subaerial environment and they have no metamorphic overprint. Moreover, their post-depositional geological histories do not seem to represent an important minerogenetic constraint since, for example, altered and unaltered pyroclastic flows and related deposits coexist in structural troughs.

Minerogenetic environments able to cause great differences in the alteration degrees of shards are those connected to percolating groundwaters and/or entrapped juvenile fluids.

The former is unlikely, due to the absence of typical structures revealing the developed hydration stages of glassy fragments such as perlitic cracks. As a consequence, entrapped fluids appear to play an important role in glassy fragment alteration. This hypothesis is strongly supported by zeolite distributions in the cooling units outcropping in the Case Oddorai sector: a large quantity of clinoptilolite, resulting from advanced shard transformations, was only found in the portions lacking degassing structures; where juvenile fluids and gases were helped to escape from the deposits along gas pipes, clinoptilolite amounts suddenly decrease (Morbidelli, 1999).

All the above considerations lead to conclude that shard alteration processes are due to interaction of the glassy matrix of undegassed pyroclastic flows with juvenile entrapped fluids.

When distributions, textural and structural relationships are considered, a different genetic model is required for zeolite occurring in epiclastic and surge deposits. The model is constrained by the presence of:

– perlitic cracks in the fine-grained crystal-glassy matrix;

– veins filled with clinoptilolite and calcite crystals;

– felt-form patches of well-developed clinoptilolite crystals grading towards unaltered matrix.

This scenario broadly agrees with fluid circulations which, mainly interacting with glassy matrix, allowed zeolite-bearing aggregates to precipitate in open spaces or veins. The presence of calcite suggests that the fluid component was related to underground water circuits moving along lithostratigraphic discontinuities. This is also supported by the position and lithostratigraphic meaning of epiclastic and base surge levels.

CONCLUSIVE REMARKS

The present study confirms that in zeolite-bearing ignimbrites, clinoptilolite is the most frequent zeolitic variety and is found bearing various textural aspects.

Minerogenetic modelling of zeolite in ash and pumice pyroclastic flows and related epiclastic deposits outcropping in northern Sardinia is constrained by several important distributive and textural aspects, identifying the following three main genetic models:

a) zeolite crystallized from entrapped fluids;

b) zeolite formed from alteration processes of glassy components from juvenile fluids;

c) zeolite formed from alteration processes of glassy components from external fluids.

The last model typifies the clinoptilolite occurring in base surge and epiclastic deposits; the others concern zeolite from ash and pumice pyroclastic flows.

The dominant role played by juvenile fluidizing components in the alteration of pyroclastic flows and zeolite crystallization is supported by several pieces of evidence.

The above minerogenetic scenario is consistent with zeolite distributions within volcanic piles and also agrees with observed geological, volcanological and petrographical features.

ACKNOWLEDGMENTS

Special thanks are expressed to Piero Brotzu who made very useful suggestions for improving the paper. Constructive reviews by B. Di Sabatino, A. Gualtieri and G. Molin are gratefully acknowledged. We thank A. Canzanella for help in electron microscopy. This research was carried out with grants from Italian CNR n° 97.00447.CT11.

REFERENCES

ALEXIEV B. and DJOUROVA E. (1988) — *Genetic features of zeolitic rocks in Bulgaria*. In «Occurrence, Properties and Utilization of Natural Zeolites», (D. Kalló and H. S. Sherry, eds), Akademiai Kiado Budapest, 77-85.

BARTH-WIRSCHING U. and HÖLLER H. (1989) — *Experimental studies on zeolite formation conditions*. Eur. J. Mineral., **1**, 489-506.

BECCALUVA L., CIVETTA L., MACCIOTTA G. and RICCI C.A. (1985) — *Geochronology in Sardinia: results and problems*. Rend. Soc. It. Min. Petr., **40**, 57-72.

BROTZU P., LONIS R., MELLUSO L., MORBIDELLI L., TRAVERSA G. and FRANCIOSI L. (1997) — *Petrology and evolution of calcalkaline magmas from the Arcuentu volcanic complex (SW Sardinia, Italy)*. Per. Mineral., **66**, 7-61.

CHERCHI A. (1985) — *Oligo-Miocene basin:* 19th European Micropaleontological Colloquium. Sardinia. Guidebook, AGIP, 87-101.

CHERCHI A. and MONTADERT L. (1982) — *The Oligo-Miocene rift of Sardinia and early history of the western Mediterranean basin,* Nature, **298**, 736-739.

DE' GENNARO M., OGGIANO G., LANGELLA A. and DI PISA A. (1995) — *Technological perspectives from volcanoclastic rocks of North Sardinia*: Proc. III Convegno Nazionale di Scienza e tecnologia delle zeoliti, Cetraro, Italy, September 28-29.

EWART (1963) — *Petrology and petrogenesis of the Quaternary pumice ash in the Taupo area, New Zealand*. J. Petrol., **4**, 392-431.

FISCHER (1963) — *Bubble wall texture and its significance*. J. Sed. Petrol., **33**, 224-227.

FISHER R.V. and SCHMINCKE H.U. (1984) — *Pyroclastic Rocks*. Springer-Verlag.

GHIARA M. R., FRANCO E., PETTI C., STANZIONE D. and VALENTINO G.M. (1993) — *Hydrothermal interaction between basaltic glass, deionized water and seawater.* Chem. Geol., **104**, 125-138.

GHIARA M. R., LONIS R., PETTI C., FRANCO E., LUXORO S., and BALASSONE G. (1997) — *The zeolitization process of Tertiary orogenic ignimbrites from Sardinia (Italy): distribution and meaning importance.* Per. Mineral., **66**, 211-231.

GHIARA M.R. and PETTI C. (1996) — *Chemical alteration of volcanic glasses and related control by secondary minerals: experimental studies.* Aquatic Geochemistry, **1**, 329-354.

GHIARA M.R., PETTI C., FRANCO R. and LONIS R. (in press) — *Distribution and genesis of zeolites in Tertiary ignimbrites from Sardinia: evidence of superimposed mineralogic processes.* In «Zeolites '97 Conference Volume»

GHIARA M. R., PETTI C., FRANCO E., LUXORO S., and GNAZZO L. (1995) — *Diagenetic clinoptilolite from pyroclastic flows of Northern Sardinia*: Proc. III Convegno Nazionale di Scienza e Tecnologia delle Zeoliti, Cetraro, Italy, September 28-29.

GHIARA M.R., PETTI C., FRANCO E., LONIS R., LUXORO S. and GNAZZO L. (1999) — *Occurrence of clinoptilolite and mordenite in Tertiary calc-alkaline pyroclastites from Sardinia (Italy).* Clays and Clay Minerals, **47**, 3, 319-328.

HAWKINS D. (1981) — *Kinetics of glass dissolution and zeolite formation under hydrothermal conditions.* Clays and Clay Minerals, **29**, 5, 331-340.

LANGELLA A., CAPPELLETTI P., CERRI G., BISH D.L. and DE' GENNARO M. (1999) — *Distribution of Industrial minerals in Sardinia: Clinoptilolite bearing rocks of the Logudoro Region.* In «Natural Microporous Materials in Environmental Technology», P. Misaelides *et al.* (eds.), 237-252.

LECCA L., CARBONI S, SCARTEDDU R., SECHI F., TILOCCA G. and PISANO S. (1986) — *Schema stratigrafico della piattaforma continentale occidentale e meridionale della Sardegna.* Mem. Soc. Geol. It., **36**, 31-40.

LECCA L., LONIS R., LUXORO S., MELIS F., SECCHI F. and BROTZU P. (1997) — *Oligo-Miocene volcanic sequences and rifting stages in Sardinia: a review.* Per. Mineral., **66**, 7-61.

LOFGREN G. (1970) — *Experimental devetrification rates of rhyolitic glass.* Geol. Soc. Am. Bull., **81**, 553-560.

LOFGREN G. (1971a) — *Spherulitic textures in glassy and crystalline rocks.* J. Geophys. Res., **76**, 5635-5648.

LOFGREN, G. (1971b) — *Experimentally produced devetrification textures in natural rhyolitic glass.* Geol. Soc. Am. Bull., **82**, 111-124.

MONTIGNY R., EDEL J. B. and THUIZAT R. (1981) — *Oligo-Miocene rotation of Sardinia: K/Ar ages and paleomagnetic data of Tertiary volcanics.* Earth Planet. Sci. Lett., **54**, 261-271.

MORBIDELLI P. (1999) — *Distribuzione, caratterizzazione e genesi delle clinoptiloliti e dei minerali associati nelle piroclastiti Terziarie della Sardegna settentrionale.* Ph. D. Thesis, University "La Sapienza", Rome, Italy.

MÜNCH P., DUPLAY J. and COCHEMÉ J.J. (1996) — *Alteration of silicic vitric tuffs interbedded in volcanoclastic deposits of the Southern Basin and Range province, Mexico: evidences for hydrothermal reactions.* Clays and Clay Minerals, **44**, 1, 49-67.

POTTER J.M. and DICKSON F.W. (1980) — *Reaction of rhyolite glass and holocrystalline basalt with NaCl solutions at 300°C; effects of time and solution composition on alteration mineralogy*: Proc. of 3rd Int. Symp. on water-rock Interaction, Canada, 170-172.

SAVELLI C., BECCALUVA L., DERIU M., MACCIOTTA G. and MACCIONI L. (1979) — *K/Ar geochronology and evolution of the Tertiary "Calc-alkalic" volcanism of Sardinia (Italy).* J. Volc. Geoth. Res., **5**, 257-280.

WIRSCHING U. (1976) — *Experiments on hydrothermal alteration processes of rhyolitic glass in closed and "open" system.* N. Jb. Miner. Mh., **5**, 203-213.

WIRSCHING U. (1981) — *Experiments on the hydrothermal formation of calcium zeolites.* Clays and Clay Minerals, **29**, 3, 171-183.